Catal Lett (2009) 129:293–302
DOI 10.1007/s10562-008-9833-6

# Characterization of $ZnAl_2O_4$ Obtained by Different Methods and Used as Catalytic Support of Pt

**Adriana D. Ballarini · Sonia A. Bocanegra ·
Alberto A. Castro · Sergio R. de Miguel ·
Osvaldo A. Scelza**

Received: 29 October 2008 / Accepted: 25 December 2008 / Published online: 17 January 2009

**Abstract** In this work the synthesis of a $ZnAl_2O_4$ spinel to be used as a support of metals and its characterization were studied. The methods used for the $ZnAl_2O_4$ preparation were: ceramic method (CM), mechanochemical synthesis in humid medium (HMS) and coprecipitation (COPR). $ZnAl_2O_4$ CM and $ZnAl_2O_4$ HMS showed negligible acidity, but the $ZnAl_2O_4$ COPR displayed a low acidity. The spinels obtained by COPR and HMS showed higher specific surface area and pore volumes than that prepared by the ceramic method. In addition the catalytic performance of Pt supported on the prepared spinel was evaluated in the *n*-butane dehydrogenation reaction. The Pt catalysts prepared with $ZnAl_2O_4$ COPR presented better activity and selectivity to olefins than the ones prepared with $ZnAl_2O_4$ HMS and $ZnAl_2O_4$ CM, which could be correlated with a higher metallic dispersion and lower particle sizes, detected by TEM. The acidity of $ZnAl_2O_4$ COPR, observed by isopropanol dehydration and TPD of pyridine, and the sequence of specific surface areas of the different spinels ($ZnAl_2O_4$ COPR > $ZnAl_2O_4$ HMS > $ZnAl_2O_4$ CM) are other important factors to define the final dispersion of the catalysts.

**Keywords** Synthesis of $ZnAl_2O_4$ support · High-energy ball milling · Platinum catalysts supported on $ZnAl_2O_4$ · Catalysts preparation and characterization

## 1 Introduction

Oxide spinels involve a large group of structurally related compounds with technological and geological properties [1]. The zinc aluminate which has a spinel structure is found in nature as a mineral named gahnite. It is a typical example of compounds of general formula $(X)[Y]O_4$, where X and Y are divalents and trivalents ions, respectively [2, 3]. It is employed as ceramic material in the secondary phase of glass in white floor ceramics to improve the resistance and mechanical properties and to preserve the whiteness. Besides, it is used like semiconductors, and in optic coating in aerospace applications [4]. Other applications of this material is as support of metals for different reactions, such as paraffins dehydrogenation, saturated alcohols dehydration to olefins, methanol and heavy alcohols synthesis, preparation of polymethylbenzenes, styrenes and acetophenones synthesis and double bound isomerization of alkenes [3]. This material seems to be a good option as catalytic support since it has a good metal dispersion capacity, low surface acidity, hydrophobic characteristics, chemical inertia and it displays high thermal stability [5]. A disadvantage of this material for catalytic applications is the low surface area, while conventional catalysts and supports are porous materials whose surface area is about 100–300 $m^2/g$ [6, 7]. The specific surface area of $ZnAl_2O_4$ can be improved choosing the appropriate synthesis method.

In general, there are several preparation methods of $ZnAl_2O_4$ spinels, for example solid state-reaction or ceramic method [3, 6–13] or wet chemical routes such as

---

A. D. Ballarini (✉) · S. A. Bocanegra · A. A. Castro ·
S. R. de Miguel · O. A. Scelza
Facultad de Ingeniería Química, Instituto de Investigaciones
en Catálisis y Petroquímica (INCAPE)-(Universidad Nacional
del Litoral)-CONICET, Santiago del Estero 2654 (3000),
Santa Fe, Argentina
e-mail: aballa@fiq.unl.edu.ar

S. R. de Miguel
e-mail: sdmiguel@fiqus.unl.edu.ar

precipitation or coprecipitation [3, 6, 7, 13–17], sol–gel [3, 6, 7, 18–21] and other methodologies like hydrothermal methods [5, 22–25], combustion in aqueous solution [26], molten salts synthesis [27], etc.

The conventional preparation method is the ceramic one [6–9, 13], which is carried out by reaction in solid phase at high temperature of gamma-alumina and zinc oxide. Other novel methods are the mechanochemical synthesis [10–12], which is a modification of the ceramic method with mechanical activation, and the coprecipitation of zinc and aluminum salts [3, 6, 7, 13–15], followed by the calcination of the obtained precursor. These techniques try to reduce the severity of the thermal treatments, thus achieving a material of higher specific area and higher chemical purity.

In this paper, the characterization of $ZnAl_2O_4$ prepared by different techniques (ceramic method, mechanochemical synthesis and coprecipitation) and the use of the obtained spinels as supports of metallic catalysts for paraffins dehydrogenation, are studied. It must be noted that the comparison of the catalytic behavior of catalysts supported on the $ZnAl_2O_4$ spinel prepared by the three methods were not previously reported in the bibliography.

## 2 Experimental

### 2.1 Preparation of $ZnAl_2O_4$

The zinc aluminate was synthesized by different ways: ceramic method (CM), mechanochemical synthesis in humid medium (HMS) and coprecipitation (COPR).

The synthesis of $ZnAl_2O_4$ by the ceramic method (CM) was carried out by a solid phase reaction between $\gamma$-$Al_2O_3$ (CK-300, 99.9%) and ZnO (AnalaR, 99.7%). The mixture was ground in a mortar and then a paste was obtained by addition of distilled water. Finally, the obtained paste was dried at 110 °C for 6 h and then calcined for 18 h at 900 °C. An excess of ZnO (5%) with respect to the stoichiometric ratio was used to assure the complete reaction.

During the mechanochemical synthesis in humid medium (HMS), $\gamma$-$Al_2O_3$ (CK-300, 99.9%) and ZnO (AnalaR, 99.7%) were mixed in a ratio of 1.05 mol ZnO/mol $\gamma$-$Al_2O_3$ and ground to a very fine powder. After grinding, distilled water was added to the powder in order to obtain a paste, which was milled during 24 h at room temperature in a ball mill. The milling process was carried out in a cylindrical vial of teflon (140 mL) containing Zirconia's balls (diameter: 13 mm). This cylinder was rotated at 200 rpm. Finally, the obtained paste was dried at 110 °C for 6 h and calcined for 12 h at 900 °C. After the preparation of the $ZnAl_2O_4$ by the two methods previously mentioned, the solids were ground to a final particle size between 35 and 80 mesh. The samples were characterized by X-ray diffraction (XRD). The diffractograms showed $ZnAl_2O_4$ and non reacted ZnO. In order to purify the spinel, eight washing steps were carried out by using 1.5 mL $g^{-1}$ of aqueous solution of $(NH_4)_2CO_3$ 1 mol $l^{-1}$, followed by washing with deionized water and drying at 120 °C for 12 h. After this, a new diffractogram was made.

The $ZnAl_2O_4$ spinel was also prepared by the coprecipitation method (COPR) with pH adjustment. Solutions of $Al(NO_3)_3 \cdot 9H_2O$ (Baker, 98.9 wt%) and $Zn(NO_3)_2 \cdot 6H_2O$ (Baker, 99.0 wt%) (stoichiometric ratio = 2 mol Al/mol Zn) were used and the pH was adjusted at 7.5 with a solution of $NH_4(OH)$ 50 v/v% in a thermal bath at 50 °C and stirring until forming a gel. After that, it was aged for 24 h. and then washed with distilled water. Then, the gel was dried at 110 °C and finally calcined at 800 °C in air flow for 8 h. To verify the structure of the solid thus obtained, the powders were characterized by X-ray diffraction (XRD).

### 2.2 Preparation of the Catalysts

For this study, Pt(0.3 wt%)/$ZnAl_2O_4$ catalysts were prepared using $ZnAl_2O_4$ synthesized by the CM, HMS and COPR methods. The catalysts were prepared by impregnation of the corresponding support with an aqueous solution of $H_2PtCl_6$. For the impregnation of $ZnAl_2O_4$ (CM), $ZnAl_2O_4$ (MSH) and $ZnAl_2O_4$ (COPR), the impregnating volume/support weight ratio was 1 mL $g^{-1}$ and the Pt concentration in the impregnating solution was 3 g $l^{-1}$, respectively. In all cases, the impregnations were carried out at room temperature for 6 h. After the impregnations, all the samples were dried at 110 °C for 12 h and calcined in air at 500 °C for 3 h.

### 2.3 Characterization of $ZnAl_2O_4$ and Catalysts

The $ZnAl_2O_4$ prepared by different ways were characterized by: X-ray diffraction (XRD), specific surface area (BET) and pore size measurements, SEM microphotographies, Fourier transform infrared spectra (FTIR), Thermogravimetric analysis (TGA), isopropanol dehydration experiments, and temperature programmed desorption (TPD) of pyridine.

X-ray diffraction experiments were performed at room temperature in a Shimadzu model XD3A instrument using CuK$\alpha$ radiation ($\lambda = 1.542$ Å), generated at 30 kV and a current of 30 mA.

The specific surface area (BET) and the pore volume of the supports prepared by different procedures were determined by a Micromeritics ASAP 2000 equipment by using $N_2$ adsorption at −196 °C. Before $S_{BET}$ measurements, samples were treated at 200 °C under high vacuum ($10^{-4}$ torr) for 2 h.

SEM microphotographies were obtained in a Microscope Jeol JSM-35C, operated at 2 kV, equipped with an acquisition system of digital images SemAfore. Samples were covered with a gold film (deposited by sputtering with a vaporizator VEECO, model VE-300, operated in Ar atmosphere) before the analysis. The measurements were carried out under the secondary electrons image mode, using 20 kV as acceleration voltage.

Fourier transform infrared spectra (FTIR) were registered in a Perkin Elmer model Spectrum One spectrometer from 4,000 to 400 $cm^{-1}$ with a resolution of 4 $cm^{-1}$. The sample (about 0.05 g) was pressed at 8 t for 5 min, to obtain an auto-supported disc.

The experiences of thermogravimetric analysis (TGA) of the precursor were performed using a DTA/TG analyzer (sDTA Mettler STARe) in an air flow of 30 mL $min^{-1}$. The samples (30 mg) were heated from room temperature up to 950 °C with a heating rate of 10 °C $min^{-1}$.

To characterize the acid properties of the $ZnAl_2O_4$ support, isopropanol dehydration experiments in a continuous flow reactor at atmospheric pressure were carried out. Prior to the reaction, samples were reduced "in situ" with $H_2$ at 530 °C. The alcohol was vaporized in a $H_2$ stream ($H_2$/isopropanol molar ratio = 19) and fed to the reactor with a space velocity of 0.52 mol alcohol $h^{-1}$ g $cat^{-1}$. The sample weight was 100 mg and the reaction temperature was 200 °C. The reaction products were analyzed by gas chromatography with a FID detector.

The acidity of the catalysts was also determined by means of temperature programmed desorption (TPD) of pyridine. An amount of 150 mg of the catalyst were first immersed in a closed vial containing pure pyridine (Merck, 99.9%) for 4 h. Then the vial was opened and the excess of pyridine was evaporated at room conditions until the surface of the particles was dry. The sample was then loaded into a quartz tube microreactor and supported over a quartz wool plug. A constant flow of nitrogen (40 mL $min^{-1}$) was passed through the sample. A first step of desorption of weakly adsorbed pyridine and stabilization was performed by heating the sample at 110 °C for 2 h. Then the temperature of the oven was raised to a final value of 450 °C at a heating rate of 10 °C $min^{-1}$. The reactor outlet was directly connected to a flame ionization detector.

The characteristics of the metallic catalysts were determined by hydrogen chemisorption, temperature programmed reduction (TPR) and Transmission Electron Microscopy (TEM).

$H_2$ chemisorption measurements were made in a volumetric equipment. The sample weight used in the experiments was 300 mg. The sample was outgassed at room temperature, heated under flowing $H_2$ (60 mL $min^{-1}$) from room temperature up to 500 °C, and then kept at this temperature for 2 h. Then, the sample was outgassed under vacuum ($10^{-4}$ torr) for 2 h. After the sample was cooled down to room temperature (25 °C), the hydrogen dosage was performed in the range of 25–100 torr. The isotherms were lineal in the range of used pressures. The chemisorbed hydrogen was calculated by extrapolation of the isotherm to pressure zero. From the data of chemisorbed $H_2$, the metallic dispersion was calculated using the formula:

$$D = \frac{n_H \cdot X \cdot MM_{Pt}}{W_{cat} \cdot C_{Pt}}$$

$n_H$ = moles of chemisorbed $H_2$; $X$ = stoichiometry of chemisorbed $H_2$ on Pt; $MM_{Pt}$ = Molar mass of Pt; $W_{cat}$ = catalyst weight; $C_{Pt}$ = Pt content.

TPR experiments were performed in a quartz flow reactor. The samples were heated at 6 °C $min^{-1}$ from room temperature up to about 700 °C. The reductive mixture (5 v/v% $H_2$–$N_2$) was fed to the reactor with a flow rate of 10 mL $min^{-1}$. Catalysts were previously calcined "in situ" at 500 °C for 3 h.

TEM measurements were carried out on a JEOL 100CX microscope with a nominal resolution of 6 Å, operated with an acceleration voltage of 100 KV, and magnification ranges of 80,000× and 100,000×. The samples, previously reduced in $H_2$ at 530 °C, were prepared by grinding, suspending and sonicating them in ethanol, and placing a drop of the suspension on a carbon copper grid. After evaporation of the solvent, the specimens were introduced into the microscope column. For each catalyst, a very important number of Pt particles was observed and the distribution curves of particle sizes were done.

### 2.4 Evaluation of the Catalytic Performance in *n*-Butane Dehydrogenation

In order to evaluate the catalytic performance of the catalysts, the *n*-butane dehydrogenation tests were carried out in a continuous flow reactor. The experiments were performed at 530 °C for 2 h in a quartz flow reactor heated by an electric furnace. The reactor (with a catalyst weight of 0.200 g) was fed with 18 mL $min^{-1}$ of the reactive mixture (*n*-butane + hydrogen, $H_2$/$n$-$C_4H_{10}$ molar ratio = 1.25). The reactive mixture was prepared "in situ" by using mass flow controllers. All gases, *n*-butane, $N_2$ (used for purge), and $H_2$ (used for the previous reduction of catalysts and for the reaction) were high purity ones (>99.99%). Prior to the reaction, catalysts were reduced "in situ" at 530 °C under flowing $H_2$ for 3 h. The reactor effluent was analyzed in a GC-FID equipment with a packed chromatographic column (1/8″ × 6 m, 20% BMEA on Chromosorb P-AW 60/80), which was kept at 50 °C during the analysis. With this analytical device, the amounts of methane, ethane, ethylene, propane, propylene, *n*-butane, 1-butene, *cis*-2-butene, *trans*-2-butene and 1,3 butadiene were measured. The *n*-butane conversion was calculated as the sum of the percentages of the chromatographic areas of all the reaction products (except $H_2$) corrected by the corresponding response factor. The selectivity to the different reaction products (i) was defined as the ratio: mol of product i/Σ mol of all products (except $H_2$). Taking into account the high temperatures used for the reaction (for thermodynamic reasons), it was necessary to determine the contribution of the homogeneous reaction. For this purpose, a blank experiment at 530 °C was performed by using a quartz bed and the results showed a negligible *n*-butane conversion ($\ll 1\%$).

## 3 Results and Discussion

### 3.1 Synthesis and Characterization of $ZnAl_2O_4$ Supports

Table 1 shows the results of specific surface (BET) and pore volume of the $ZnAl_2O_4$ prepared by the different methods. The specific surface of the support obtained by coprecipitation is higher than that of the $ZnAl_2O_4$ obtained by the mechanochemical synthesis in humid medium, and much higher than that of the spinel prepared by ceramic method. Similar tendencies are observed for the pore volumes of the different spinels. This effect can be correlated with the different severity of the thermal treatments used for the three synthesis methods. In fact, the material obtained by CM has a low specific surface area and pore volume since long-lasting high temperatures were used during the preparation.

Figures 1, 2 and 3 shows the X-ray diffraction measurements of the $ZnAl_2O_4$ prepared by the ceramic method (CM), before (a) and after (b) the purification treatments, by the mechanochemical synthesis in humid medium (HMS), before (a) and after (b) the purification treatments, and by the coprecipitation (COPR) technique, precursor (a) and final product (b), respectively. In Figs. 1a and 2a, DRX diffractograms show the presence of $ZnAl_2O_4$ (JCPDS file 05-0669) and traces of ZnO (JCPDS file 36-1451) at the end of the synthesis methods named CM and HMS. After purification with $(NH_4)_2CO_3$, ZnO species are completely eliminated, such as Figs. 1b and 2b display, thus remaining only the structure of $ZnAl_2O_4$. In the case of the spinel prepared by HMS, the signals corresponding to ZnO are smaller than those obtained by the ceramic method, thus indicating that in the first case a more intimate contact (due to the intensive milling) would favour the reaction between ZnO and $Al_2O_3$. In Fig. 3a it is observed the diffractogram of the precursor obtained by the coprecipitación synthesis (COPR), which is very amorphous, while in Fig. 3b, only the structure of $ZnAl_2O_4$ is detected. Hence, the use of the coprecipitation synthesis leads to a pure final product, without the presence of other compounds like ZnO, as happens with the mechanochemical and ceramic methods.

From the XRD data, the mean crystal sizes of the spinels prepared by the different methods were obtained by means of the Scherrer equation. By analyzing the diffractograms, it was observed that the wideness of the diffraction peaks of the spinel decreased and its intensity increased when higher temperatures and calcinations times were used. In

**Table 1** Measurements of specific surface and pore volume of the $ZnAl_2O_4$ prepared by different methods

| | CM | HMS | COPR |
|---|---|---|---|
| Specific surface (BET) ($m^2$/g) | 11 | 21 | 40 |
| Pore volume (mL/g) | 0.026 | 0.053 | 0.118 |

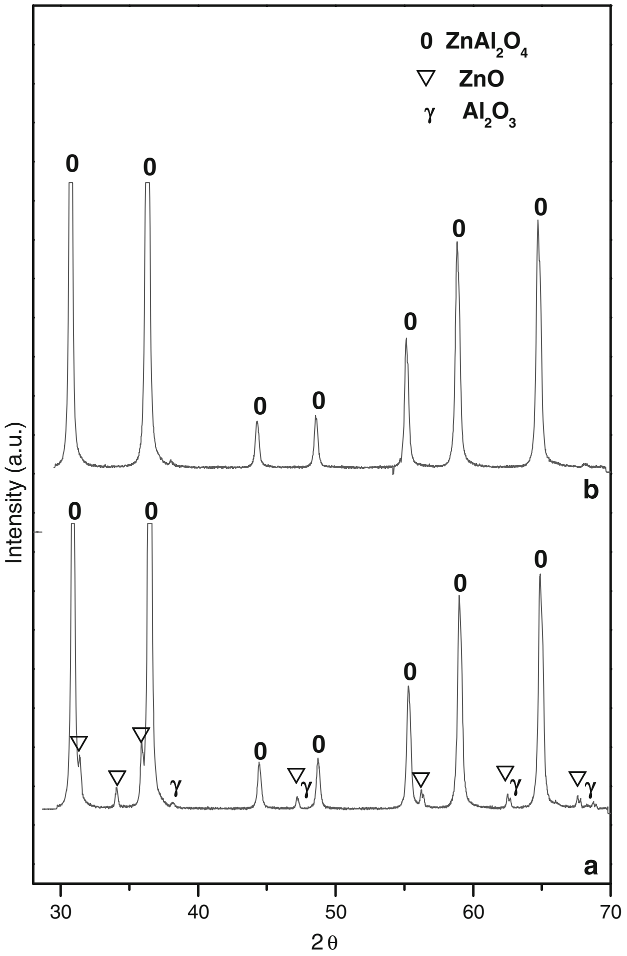

**Fig. 1** X-ray diffractograms of spinels prepared by CM, before (**a**) and after (**b**) the purification treatments

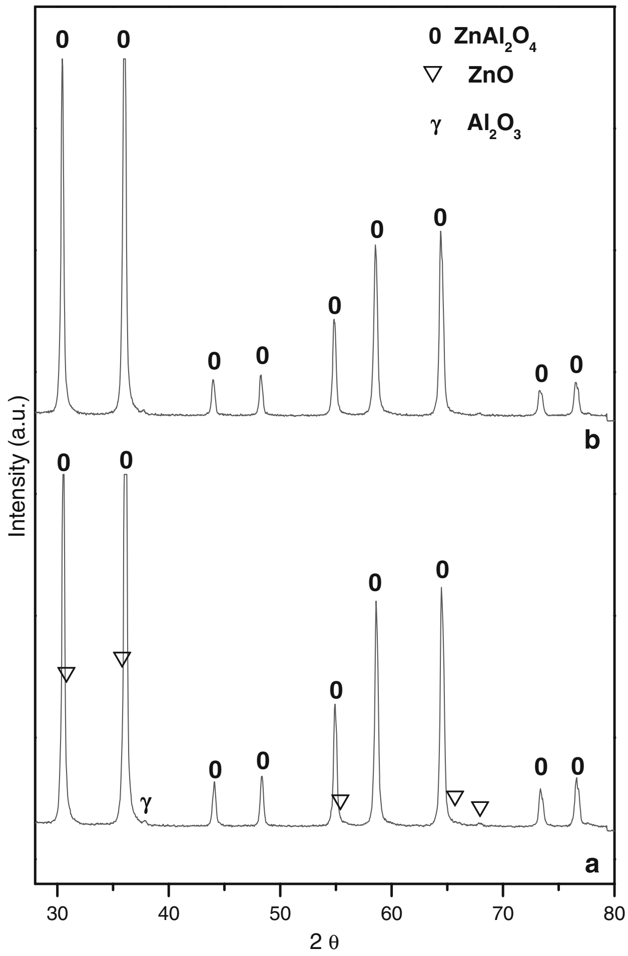

**Fig. 2** X-ray diffractograms of spinels prepared by HMS, before (**a**) and after (**b**) the purification treatments

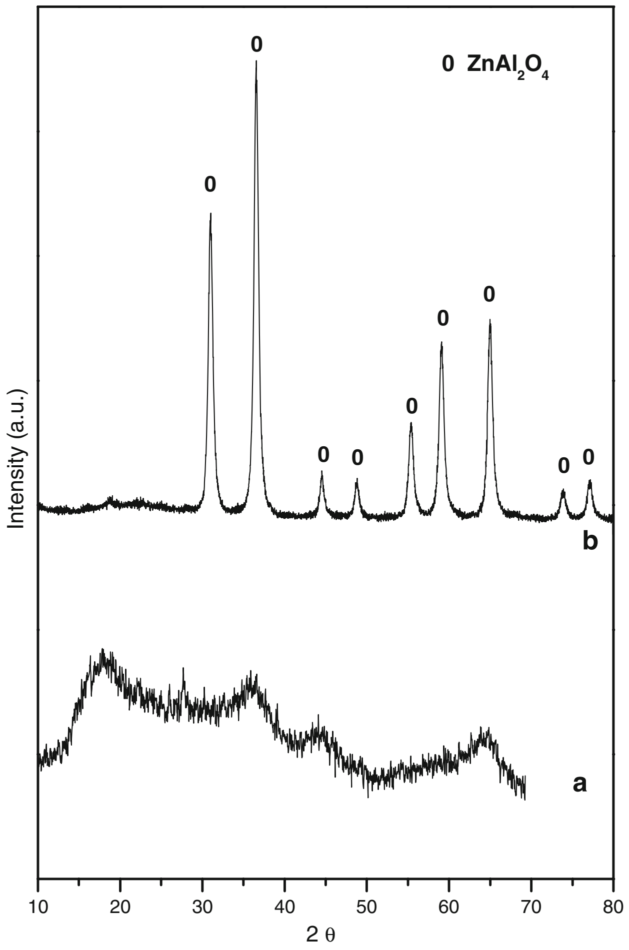

**Fig. 3** X-ray diffractograms of spinels prepared by COPR: **a** Precursor. **b** Final product

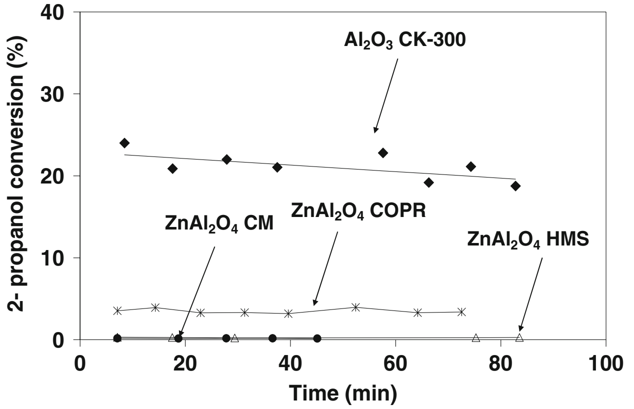

**Fig. 4** Isopropanol conversion vs. reaction time for the different $ZnAl_2O_4$ spinels and $\gamma$-$Al_2O_3$ (reference)

fact, the crystal sizes (Φ) of the spinels decreased with the decrease of the severity of the thermal treatment used for the synthesis, following this sequence:

$$ZnAl_2O_4\ \mathrm{CM}\ (\Phi = 33\,\mathrm{nm}) > ZnAl_2O_4\ \mathrm{HMS}\ (\Phi = 20\,\mathrm{nm}) > ZnAl_2O_4\ \mathrm{COPR}\ (\Phi = 15\,\mathrm{nm})$$

The acid properties of $ZnAl_2O_4$ prepared by different methods were determined by comparing the 2-propanol dehydration capacities of these materials with that of $\gamma$-$Al_2O_3$ (taken as reference). Results are shown in Fig. 4. The reaction produces propylene (in high concentration) and small amounts of di-isoproylether. It must be noted that $\gamma$-$Al_2O_3$ shows Lewis acidity [28] and an important dehydration conversion (about 20%). Experiments of isopropanol dehydration confirm the non-acidic characteristics of $ZnAl_2O_4$ spinels prepared by CM and HMS since they have practically negligible conversions (<0.5%). These results agree with others reported in the bibliography about the neutral characteristics of the $ZnAl_2O_4$ [29]. However the spinel prepared by coprecipitation displays low acidity since the 2-propanol conversion reaches about 3%.

In order to confirm that the acidity of the spinel prepared by COPR is higher than those prepared by the other

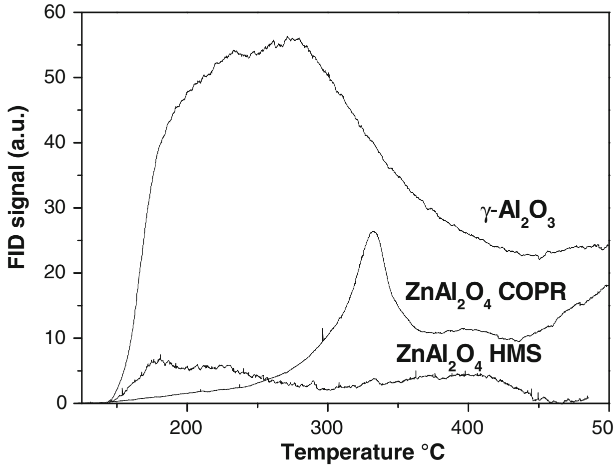

**Fig. 5** Desorption profiles of pyridine on the spinels (COPR and HMS) and on $\gamma$-$Al_2O_3$ (reference)

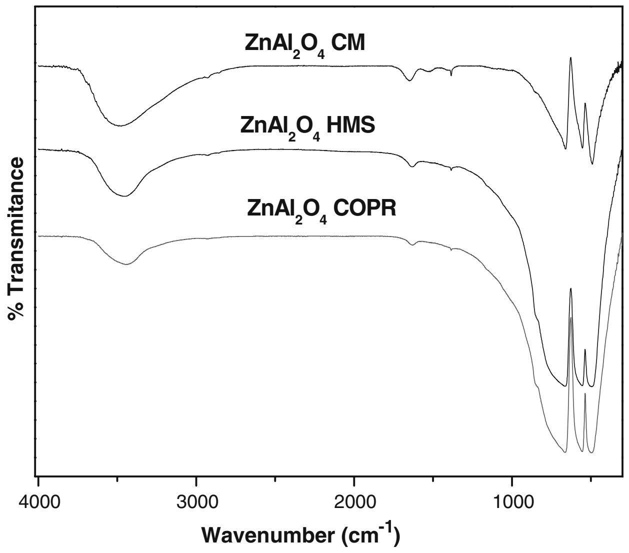

**Fig. 6** FTIR spectra of $ZnAl_2O_4$ prepared by the CM, HMS and COPR methods

methods, experiments of pyridine temperature programmed desorption (Py-TPD) were carried out, and the results are shown in Fig. 5. Although the spinels HMS and COPR display much lower pyridine desorption and hence much lower acidity than $\gamma$-$Al_2O_3$, $ZnAl_2O_4$ HMS shows negligible acid characteristics while $ZnAl_2O_4$ COPR is a slightly acidic material. In this sense, while the TPD profile of $ZnAl_2O_4$ COPR displays a sharp peak at 325 °C and a wide desorption region at higher temperatures, the one corresponding to $ZnAl_2O_4$ HMS is practically negligible. The quantification of total acid sites, obtained by integrating the normalized Py-TPD profiles, shows that $ZnAl_2O_4$ COPR and $ZnAl_2O_4$ HMS has 35 and 9%, respectively, of the total acid sites of the $\gamma$-$Al_2O_3$ used as reference. A comparison of the total acid sites referred to the specific surface area of the differents supports follows a similar sequence: $\gamma$-$Al_2O_3$ > $ZnAl_2O_4$ COPR > $ZnAl_2O_4$ SMH. The presence of a low acidity in $ZnAl_2O_4$ COPR would be due to a little excess of aluminium (respect to the stoichiometric ratio), which could be present inside the $ZnAl_2O_4$ spinel structure or segregated. This hypothesis was also suggested by Armendariz et al. for $MgAl_2O_4$ spinel with an excess of Al respect to the Al/Mg stoichiometric ratio [30].

FTIR spectra of the $ZnAl_2O_4$ spinels prepared by the three methods, shown in Fig. 6, are very similar between them, displaying an intense band around 3,450 $cm^{-1}$, which is attributed to the vibration of the OH groups bonded to the surface. All the samples also show bands between 1,400 and 1,600 $cm^{-1}$, the first one associated to the vibrations Al–OH, characteristics of the $ZnAl_2O_4$, and the second one to the HOH due to the water [7]. The bands around 900–400 $cm^{-1}$ would be related to the inorganic network [31].

Thermogravimetric Analysis (TGA) experiments were also carried out on the three spinel precursors. Figure 7a displays the results of the Thermogravimetric analysis (TGA and its derivative, dTGA) of the mixture (obtained by milling with a mortar—ceramic method) between ZnO and $\gamma$-$Al_2O_3$. The total weight loss was about 10%. The dTGA profile shows peaks at 58 and 171 °C, corresponding to the release of free bound water, and another one at 258 °C. This last peak would correspond to the loss of crystal water from the reactives, since the dTGA profile corresponding to pure ZnO displays an important peak at 260 °C and that of $\gamma$-$Al_2O_3$ shows a small one at similar temperature.

The results of the thermal gravimetric analysis (TGA and dTGA) of the mixture (obtained by wet milling in ball mill—mechanochemical synthesis) between ZnO and $\gamma$-$Al_2O_3$ are shown in Fig. 7b. The total weight loss was about 13%. The dTGA profile shows peaks at 77 °C, corresponding to the release of free bound water, another one at 160 °C and a small one at 260 °C. The profile of the mixture submitted to a severe wet milling is different from the profiles of the pure reactives, mainly for the appearance of a new and important peak at 160 °C, which could be due to the loss of crystal water from a new compound originated by the hydration process of the mixture between alumina and zinc oxide during the intense milling for 12 h [32]. However, this new compound was not observed by XRD determination (Fig. 3b) probably due to a very amorphous structure and to a very low concentration.

Finally, Fig. 7c displays the results of the thermal gravimetric analysis (TGA and dTGA) of the spinel precursor obtained by coprecipitation. The total weight loss is about 70%, thus indicating a low yield during the production of $ZnAl_2O_4$ by the coprecipitation method. In the dTGA profile, small peaks at 75 °C and 141 °C (corresponding to the release of free bound water), and main ones

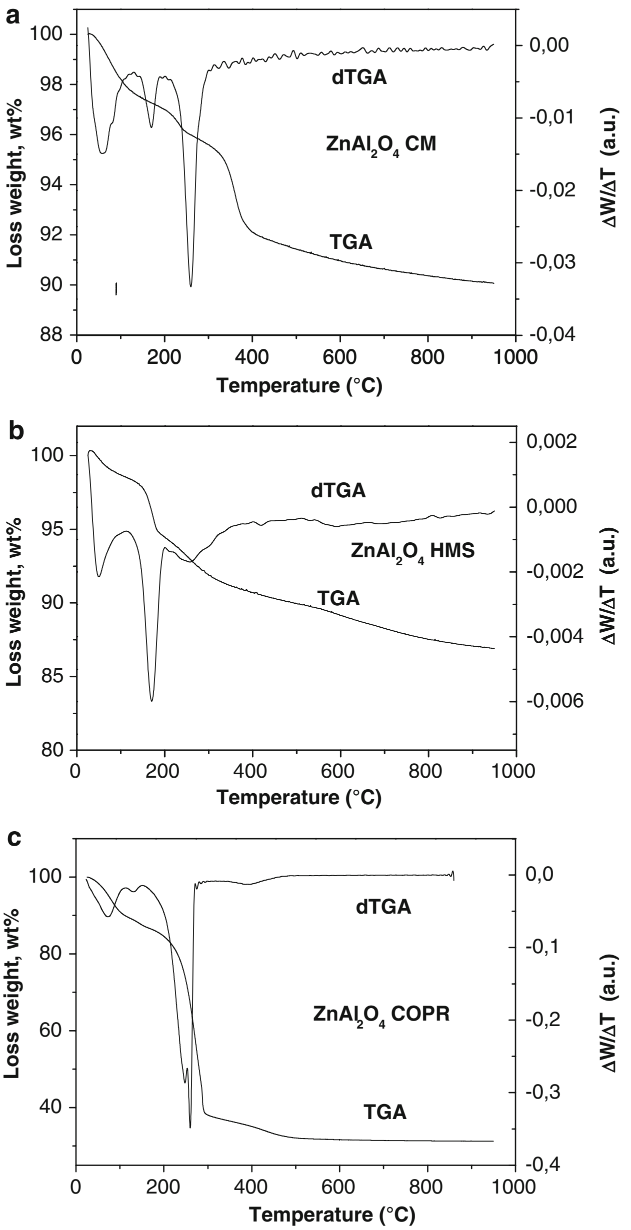

**Fig. 7** Results of the gravimetric thermal analysis (TGA and dTGA-derivative of TGA) of the: **a** Mixture between ZnO and $\gamma$-$Al_2O_3$ ground in mortar (ceramic method). **b** Mixture between ZnO and $\gamma$-$Al_2O_3$ submitted to a wet milling during 24 h (mechanochemical synthesis). **c** Precursor obtained by the coprecipitation method

with maxima at 268 and 296 °C, are observed. These last peaks would correspond to the decomposition of residual nitrates and crystallization water, and to the dehydroxilation process.

TGA experiments did not give additional information about the $ZnAl_2O_4$ spinel formation at high temperatures in all cases, due probably to the slowness of the transformation process of the precursors into the spinel. However, this fact could cause the small weight losses observed in TGA experiments at high temperatures.

Figure 8a and b show the SEM microphotographs of the different materials involved in the different steps of the ceramic method. Figure 8a displays the microstructure of the mixture between ZnO and $\gamma$-$Al_2O_3$ after the milling in a mortar, thus showing large particles. After the calcination treatment to produce the spinel structure, agglomerations of globular-shaped particles and with sizes smaller than those of the mixture of reactives, are observed in Fig. 8b. Figure 8c and d show the SEM microphotographs of the different materials involved in the mechanochemical synthesis. Figure 8c displays the microstructure of the mixture between ZnO and $\gamma$-$Al_2O_3$ after the wet milling in a ball mill. After the calcination treatment (Fig. 8d), the spinel shows a structure similar to that of Fig. 8b. Finally, Fig. 8e and f show the SEM microphotographs of the different materials involved in the coprecipitation method. Particles with a laminar structure are observed in Fig. 8e for the precursor, while after the calcination at 800 °C, the structure of the spinel is similar to the others (shown in Fig. 8b and d), thus showing agglomerations of particles with a globular shape (Fig. 8f).

## 3.2 Characterization and Evaluation in *n*-Butane Dehydrogenation of Pt/$ZnAl_2O_4$

Pt (0.3 wt%) catalysts supported on the three $ZnAl_2O_4$ spinels were characterized by hydrogen chemisorption and temperature programmed reduction (TPR), and evaluated in *n*-butane dehydrogenation reaction. Table 2 shows the results of $H_2$ chemisorption of the three catalysts. Pt/$ZnAl_2O_4$ CM displays lower metallic dispersion than both Pt/$ZnAl_2O_4$ HMS and Pt/$ZnAl_2O_4$ COPR, in agreement with the fact that the $ZnAl_2O_4$ COPR has a specific surface area higher than $ZnAl_2O_4$ HMS and much higher than $ZnAl_2O_4$ CM. The presence of a spinel with a very low surface area like that obtained by ceramic method leads to a support with lower capacity to disperse the metallic phase, even at low Pt concentrations (0.3 wt%).

Besides, the catalytic performances of Pt supported on the spinels prepared by the different methods were evaluated in the *n*-butane dehydrogenation reaction in continuous flow. Figure 9 shows the catalytic activity of the different Pt (0.3 wt%) catalysts supported on spinels prepared by the CM, HMS and COPR methods as a function of the reaction time. Moreover, Table 2 shows the selectivity (S) values to butenes and the yield (Y) to butenes (defined as the product of the conversion and the selectivity to all butenes). Higher conversions (Fig. 9) and selectivities to butenes (Table 2) are observed for the catalyst supported on $ZnAl_2O_4$ prepared by coprecipitation, which would be due to a better Pt dispersion on a spinel with a higher specific surface area. In fact, the metallic dispersion (D) of the monometallic catalysts decreases in the following way:

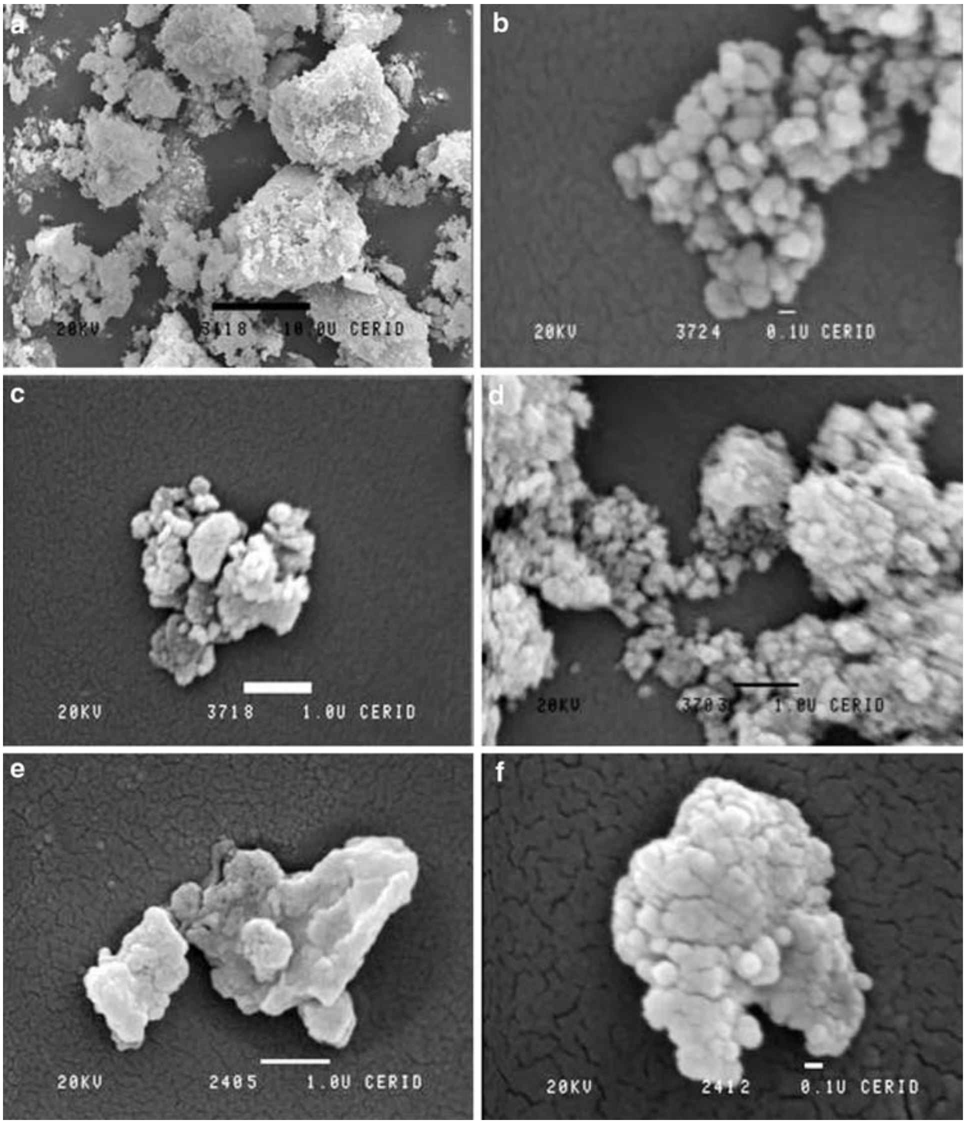

**Fig. 8** SEM microphotographies of materials involved in: ceramic method **a** ZnO and $\gamma$-$Al_2O_3$ ground in mortar. **b** $ZnAl_2O_4$; mechanochemical synthesis. **c** ZnO and $\gamma$-$Al_2O_3$ submitted to wet milling. **d** $ZnAl_2O_4$; and coprecipitation method. **e** Precursor. **f** $ZnAl_2O_4$

**Table 2** Hydrogen chemisorbed (H) and Pt dispersion

| Catalysts | H ($\mu$mol $g^{-1}$) | Dispersion (%) | $S^0$* | $S^f$* | $Y^0$* | $Y^f$* |
|---|---|---|---|---|---|---|
| Pt(0.3%)/$ZnAl_2O_4$ CM | 1.48 | 19.2 | 73.7 | 92.1 | 3.8 | 4.6 |
| Pt(0.3%)/$ZnAl_2O_4$ HMS | 1.98 | 25.7 | 88.2 | 90.4 | 8.06 | 6.40 |
| Pt(0.3%)/$ZnAl_2O_4$ COPR | 2.23 | 40.0 | 91.8 | 94.3 | 16.9 | 12.7 |

Behaviour in the *n*-butane dehydrogenation: Intial and final selectivities ($S^0$ and $S^f$) and yields ($Y^0$ and $Y^f$) to butenes for the different monometallic catalysts

* $S^0$ and $Y^0$, taken at 10 min reaction time; $S^f$ and $Y^f$, taken at 120 min reaction time

$$Pt/ZnAl_2O_4COPR(D{=}40\%) > Pt/ZnAl_2O_4HMS(D{=}26\%) > Pt/ZnAl_2O_4CM(D{=}19\%)$$

Besides, the yield of the catalysts to the different butenes (Table 2) followed a sequence similar to that of the butane conversion and the metallic dispersion. In this sense, the catalyst supported on $ZnAl_2O_4$ COPR showed the highest yield to olefins. The final yield to butenes of the Pt/$ZnAl_2O_4$ COPR (13%) are higher than others reported in the literature such us Pt/$Al_2O_3$ (5%) and Pt/$Al_2O_3$-Na (9%) [33].

Taking into account the results found both in the dehydrogenation reaction and in $H_2$ chemisorption, it was

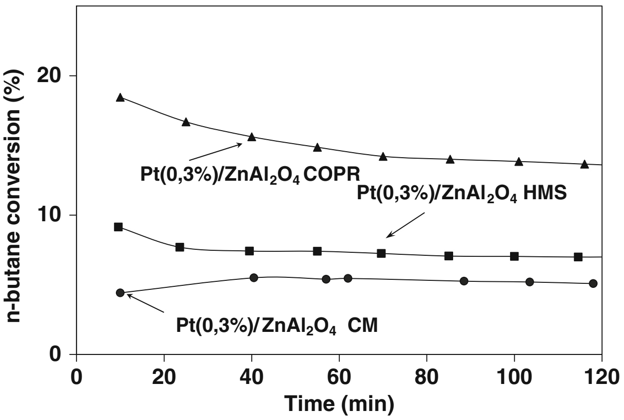

**Fig. 9** *n*-Butane conversion vs. reaction time for Pt catalysts supported on $ZnAl_2O_4$ prepared by the CM, HMS and COPR methods. ($T = 530$ °C, $W_{cat} = 0.200$ g, $H_2/n\text{-}C_4H_{10} = 1.25$)

decided to study with more details the state of the metallic phase in the three monometallic catalysts. Hence, a characterization by Temperature Programmed Reduction (TPR) and Transmission Electron Microscopy (TEM), were carried out.

TPR profiles of the three catalysts are displayed in Fig. 10. $Pt/ZnAl_2O_4$ HMS and $Pt/ZnAl_2O_4$ CM show a reduction peak located at 250–260 °C, while the peak of $Pt/ZnAl_2O_4$ COPR is wider and appears at about 300 °C. The existence of this reduction zone was also observed in Pt catalysts supported on alumina, and they can be due to the reduction of oxychlorinated Pt compounds originated during the impregnation of $H_2PtCl_6$ and in subsequent thermal treatments [34]. These TPR results indicate small differences in the Pt reducibility between the three catalysts.

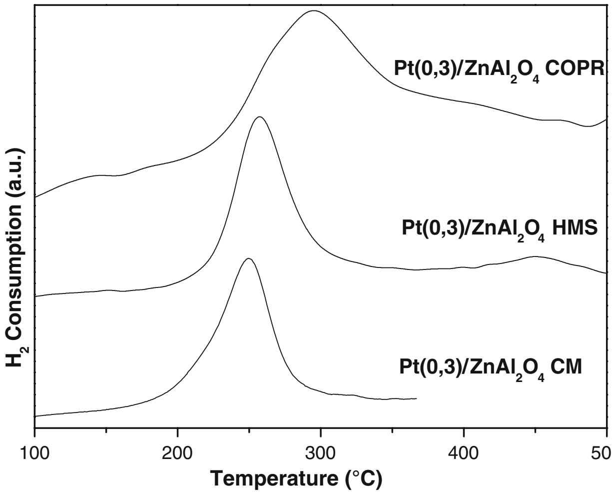

**Fig. 10** TPR profiles of Pt catalysts supported on $ZnAl_2O_4$ prepared by the CM, HMS and COPR methods

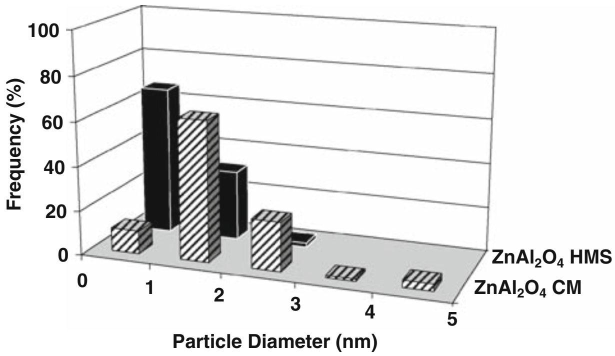

**Fig. 11** Distribution of particle sizes by TEM in Pt catalysts supported on $ZnAl_2O_4$ prepared by the CM and HMS

Figure 11 shows the distribution of metallic particle sizes (detected by TEM) corresponding to Pt catalysts supported on the $ZnAl_2O_4$ CM and $ZnAl_2O_4$ HMS. The catalyst supported on the $ZnAl_2O_4$ CM has Pt particles with sizes between 1 and 2 nm (11%), between 2 and 3 nm (63%), between 3 and 4 nm (22%) and other higher than 4 nm (4%). The mean particle diameter of this catalyst is 2.86 nm. The characterization by TEM of the $Pt/ZnAl_2O_4$ HMS shows a lower mean particle diameter (1.91 nm), having Pt particles with sizes between 1 and 2 nm (67%), between 2 and 3 nm (31%), and others between 3 and 4 nm (only 2%). Finally, it was impossible to detect particles by TEM in the Pt catalyst supported on $ZnAl_2O_4$ COPR, which means that the particle sizes are lower than 1.5 nm. These results are in agreement with the higher dispersion values obtained for the $Pt/ZnAl_2O_4$ COPR catalyst by $H_2$ chemisorption, and they could be related with the higher acidity of $ZnAl_2O_4$ COPR, observed by isopropanol dehydration and TPD of pyridine. Hence during the metallic impregnation, the $ZnAl_2O_4$ COPR spinel would be able to adsorb anions (like $PtCl_6^{2-}$) with a higher interaction, thus leading probably to higher metallic dispersions. Moreover the sequence of specific surface areas (Table 1) of the different spinels ($ZnAl_2O_4$ COPR > $ZnAl_2O_4$ HMS > $ZnAl_2O_4$ CM) is another important factor to define the final dispersion of the catalysts.

## 4 Conclusions

- The presence of a spinel with a very low surface area like that obtained by the conventional ceramic method leads to a material with lower capacity to achieve high dispersions of the metallic phase, even at low metallic concentrations.
- The mechanochemical synthesis is a novel technique that is appropriate to obtain spinels with a higher

specific surface area than with the conventional ceramic method.

- The coprecipitation synthesis seems to be appropriate to synthesize solids with the adequate characteristics for application as support of metallic catalysts for *n*-butane dehydrogenation: high chemical purity, higher specific area and an adequate acidity (necessary to favour the interaction between the metallic precursor and the support during the impregnation step).
- The higher acidity of $ZnAl_2O_4$ COPR, observed by isopropanol dehydration and TPD of pyridine, and the sequence of specific surface areas of the different spinels ($ZnAl_2O_4$ COPR > $ZnAl_2O_4$ HMS > $ZnAl_2O_4$ CM) is another important factor to define the final dispersion of the catalysts.
- The Pt catalysts prepared with $ZnAl_2O_4$ COPR presented better activity and selectivity (in the reaction of *n*-butane dehydrogenation) than the ones prepared with $ZnAl_2O_4$ HMS and $ZnAl_2O_4$ CM, which could be correlated with a higher metallic dispersion and lower particle sizes, detected by $H_2$ chemisorption and TEM, respectively.

**Acknowledgments** Authors thank Miguel A. Torres for the experimental assistance, to Dra. Silvana A. D'Ippolito for TPD of pyridine experiments and to M. J. Yañez (CCT-Bahía Blanca) for TEM measurements. Besides, this work was made with the financial support of Universidad Nacional del Litoral and CONICET—Argentina.

## References

1. Vicenzini P (ed) (1987) High tech ceramics. Elsevier, Amsterdam
2. Phani AR, Passacantando M, Santucci S (2001) Mater Chem Phys 68:66–71
3. van der Laag NJ, Snel MD, Magusin PC, de With G (2004) J Eur Ceram Soc 24:2417–2424
4. Qivastar Inc. Ridgeerest, CA, and Hugest Space Communication Co, El Segundo; CA, US Patent No 5820669, 13 October 1998
5. Zawadzki M (2006) Solid State Sci 8:14–18
6. Valenzuela M, Jacobs J, Bosch P, Reijne S, Zapata B, Brongersma H (1997) Appl Catal A: Gen 148:315–324
7. Valenzuela MA (1990) Thesis, ESIQIE-IPN, México
8. Strohmeier B, Hercules D (1984) J Catal 8:266–279
9. Ganesh I, Srinivas B, Saha B, Johnson R, Mahajan Y (2004) J Eur Ceram Soc 24:201–207
10. Zdujié MV, Milosevié OB (1992) Mater Lett 13:125–129
11. Domanski D, Urretavizcaya G, Castro F, Gennari F (2004) J Am Ceram Soc 87:2020–2024
12. Kong LB, Huang JM (2002) Mater Lett 56:238–243
13. El-Nabharawy T, Attia A, Alaya M (1995) Mater Lett 24:319–325
14. Aguilar-Rios G, Valenzuela MA (1992) Appl Catal A: Gen 90:25–34
15. Armendariz H, Guzmán A, Toledo A, Llanos M, Vazquez A, Aguilar G (2000) In: Morfao J, Faria J, Figueiredo J (eds) Proc. XVII Iberoamerican symposium of catalysis. Porto, pp 105–114
16. Li JG, Ikegami T, Lee J, Mori T, Yamija Y (2001) Ceram Int 27:481–489
17. Li J, Ikegami T, Lee J, Mori T, Yajima Y (2001) J Eur Ceram Soc 21:139–148
18. Guo J, Lou H, Wang X, Zheng X (2004) Mater Lett 58:1920–1923
19. Chen L, Sun X (2004) J Alloys Compd 376:257–261
20. Wu Y, Du J, Leong Choy K, Hench L, Guo J (2005) J Thin Solid Film 472:150–156
21. Monrós G, Tena J (1995) J Mater Chem 5:85–90
22. Wrzyszcz J, Zawadzki M (2002) J Mol Catal A: Chem 189:203–210
23. Zawadzki M, Mista W, Kepinski L (2001) Vacuum 63:291–296
24. Chen Z, Shi E (2002) Mater Lett 56:601–605
25. Yang CC, Chen SY, Cheng SY (2004) Powder Technol 148:3–6
26. Mimani T (2001) J Alloys Compd 315:123–128
27. Li Z, Zhang S, Lee W (2007) J Eur Ceram Soc 27:3407–3412
28. Pines H, Haag W (1960) J Am Chem Soc 82:2471–2478
29. Pakhomov NA, Buyanov RA (1995) Stud Surf Sci Catal 91:1101–1110
30. Armendariz H, Guzman A, Toledo J, Llanos M, Vazquez A, Aguilar-Rios G (2001) Appl Catal A 211:69–80
31. Barroso M, Gomez M, Andrade Gamboa J, Arrúa L, Abello M (2006) J Phys Chem Solids 67:1583–1589
32. Ye G, Troczynski T (2006) Ceram Int 32:257–262
33. Bocanegra S, Castro A, Guerrero-Ruiz A, Scelza O, de Miguel A (2006) Chem Ing J 118:161–166
34. de Miguel S, Bocanegra S, Vilella IJ, Guerrero-Ruiz A, Scelza O (2007) Catal Lett 119:5–15